

## Thickness dependence of the MoO<sub>3</sub> blocking layers on ZnO nanorod-inverted organic photovoltaic devices

Mingjun Wang,<sup>1,2</sup> Yuan Li,<sup>1</sup> Huihui Huang,<sup>1,2</sup> Eric D. Peterson,<sup>1</sup> Wanyi Nie,<sup>1</sup> Wei Zhou,<sup>1</sup> Wei Zeng,<sup>2</sup> Wenxiao Huang,<sup>1</sup> Guojia Fang,<sup>2,a)</sup> Nanhai Sun,<sup>2</sup> Xingzhong Zhao,<sup>2</sup> and David L. Carroll<sup>1,a)</sup>

<sup>1</sup>Department of Physics, Center for Nanotechnology and Molecular Materials, Wake Forest University, Winston-Salem, North Carolina 27109, USA

<sup>2</sup>Key Laboratory of Acoustic and Photonic Materials and Devices of Ministry of Education and Department of Electronic Science and Technology, School of Physical Science and Technology, Wuhan University, Wuhan 430072, People's Republic of China

(Received 6 August 2010; accepted 20 January 2011; published online 10 March 2011)

Organic solar cells based on vertically aligned zinc oxide nanorod arrays (ZNR) in an inverted structure of indium tin oxide (ITO)/ZNR/poly(3-hexylthiophene): (6,6)-phenyl C61 butyric acid methyl ester (P3HT:PCBM)/MoO<sub>3</sub>/aluminum (Al) were studied. We found that the optimum MoO<sub>3</sub> layer thickness condition of 20 nm, the MoO<sub>3</sub> can effectively decrease the probability of bimolecular recombination either at the Al interface or within the active layer itself. For this optimum condition we get a power conversion efficiency of 2.15%, a short-circuit current density of 9.02 mA/cm<sup>2</sup>, an open-circuit voltage of 0.55V, and a fill factor of 0.44 under 100 mW/cm<sup>2</sup> irradiation. Our investigations also show that the highly crystallized ZNR can create short and continuous pathways for electron transport and increase the contact area between the ZNR and the organic materials. © 2011 American Institute of Physics. [doi:10.1063/1.3554381]

Photovoltaic (PV) devices based on conjugated polymers such as poly(3-hexylthiophene) (P3HT) and (6,6)-phenyl C61 butyric acid methyl ester (PCBM) have attracted a lot of attention in recent years because they are easily fabricated. This offers the possibility of solar cells that are cost-effective, flexible, and of large area. However, the strong acidic nature of the poly(3,4-ethylene dioxythiophene):(poly-styrene sulfonic acid) (PEDOT:PSS) modified layer, can lead to corrosion of the indium tin oxide (ITO) electrode<sup>1</sup> and degradation of the conjugated polymer in the active layer. Several groups have constructed inverted structure PV devices with highly transparent metal oxides, i.e., TiO<sub>x</sub> (Refs. 2 and 3) or ZnO (Refs. 4 and 5) on the transparent electrode as the cathode buffer layer. ZnO is a good candidate for this application because it is a cheap and environmentally friendly material that can be synthesized with high purity and crystallinity at low temperature. Its high electron mobility and high transparency in the visible-wavelength range allow it to be both an effective electron transporter and excellent wave guide. Olson *et al.* have reported efficient ZnO/polymer devices with different ZnO morphologies.<sup>6,7</sup> Vertically oriented ZnO nanorods arrays (ZNR) can provide continuous electron transport pathways. Moreover, the high surface-to-volume of the vertically aligned ZNR can ensure three-dimensional contact with the polymer and provide many direct electrical pathways to transport electrons to the cathode directly. Vishal Shrotriya *et al.* have verified that MoO<sub>3</sub> can replace PEDOT:PSS as the hole selective layer, which can be conveniently deposited by evaporation before depositing the anode metal.<sup>8</sup> The thickness of the MoO<sub>3</sub> hole selective layer is a vital parameter in the inverted solar cell structure. To further understand the effect of MoO<sub>3</sub> thickness on the ZNR-based invert structures, layers of various thick-

nesses were deposited onto a series of inverted ZNR solar cells by thermal evaporation. We found the thickness of the MoO<sub>3</sub> layers had a significant effect on the performance of the inverted ZNR solar cells.

The ZNR-based inverted solar cell was fabricated by the normative process as illustrated in Fig. 1. Devices were fabricated on precleaned and etched conducting ITO [Delta Technologies,  $R_s=10 \Omega \text{ sq}^{-1}$  (Delta Technologies Ltd, Stillwater, Minnesota)] coated glass substrates. A 130 nm P3HT:PCBM (1:0.8 Weight ratio, 15 mg/ml in chlorobenzene) layer was spin-cast on top of pregrown ZNR<sup>9</sup> substrates. Different thicknesses of MoO<sub>3</sub> were deposited and capped with a 100 nm Al by thermal evaporation ( $5 \times 10^{-6}$  torr) with a shadow mask. The devices were then annealed under N<sub>2</sub> ambient at 150 °C for 7 min. The PV characteristics were measured with a Keithley 236 source-measurement unit under 100 mW/cm<sup>2</sup> using an AM 1.5G standard Newport #96000 Solar Simulator. The external quantum efficiency (EQE) was measured using a Newport Cornerstone 260 Monochromator in conjunction with a Newport 300W Xenon light source, and a Merlin Lock-In amplifier. The morphology analysis of the ZNRs and solar cell

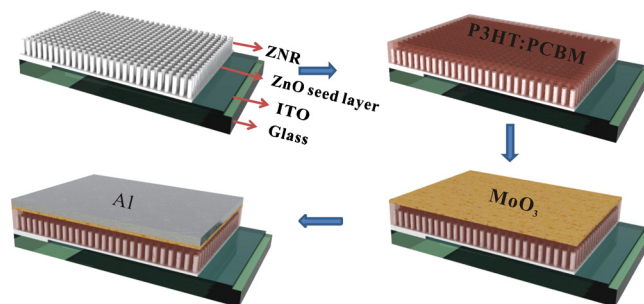


FIG. 1. (Color online) Schematic illustration of the fabrication process of ZNR based bulk heterojunction (BHJ) solar cells.

<sup>a)</sup>Electronic mail: carrolldl@wfu.edu. Tel: +1-(336) 727-1806.

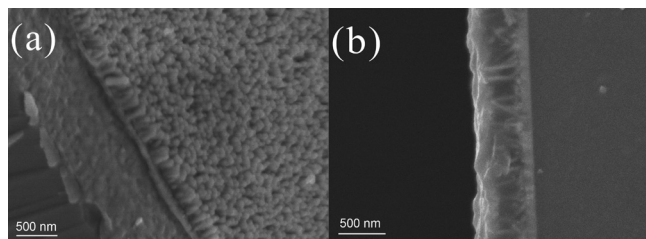


FIG. 2. (a) The side view SEM images of the ZNRs grown by the hydrothermal method and (b) cross sectional views of the P3HT:PCBM-coated ZNRs.

composite structure were done with a scanning electron microscope [JEOL, JSM-6330F (JEOL Ltd, Tokyo, Japan)].

Figure 2(a) shows ZNRs approximately 120 nm in length that are grown on a 100 nm ZnO seed layer. The ZNRs form a highly organized structure with the rods forming perpendicular to the seed layer in closely packed formation, leading to a rough surface. From Fig. 2(b) we can see that P3HT:PCBM formed an even coating on top of the ZNRs, and the infiltrated well between the rods.

Figure 3(a) shows the  $J$ - $V$  curve of devices without (0 nm: device A) and with 5, 10, 15, 20, and 25 nm MoO<sub>3</sub> blocking layer (devices B, C, D, E, and F, respectively), we can see that with the increased thickness of the MoO<sub>3</sub> layer, the short-circuit current density ( $J_{sc}$ ) increased from 5.25 to 9.02 mA/cm<sup>2</sup>. It should be noted that the surface roughness of the ZNR array is much larger than a spin coated sol gel based ZnO film. This led us to use very slow spinning speeds to ensure a reasonably even coating of polymer-fullerene solution on the rods. However, the surface of the active layer was still not smooth enough for a 15 nm or less MoO<sub>3</sub> layer to form a consistent film. For devices B and C, the MoO<sub>3</sub> layer can only cover the top of each rod and the bottom well between two ZnO nanorods, leaving the aluminum capping layer in direct contact with the polymer at the sides of the rods. This means that the MoO<sub>3</sub> is only partially effective as an hole transport layer. Due to the similar conduction band edge of ZnO and Al, the electron can jump from the lowest unoccupied molecular orbital of PCBM to either the conduction band of the Al or the ZnO. This decrease in electrode

selectivity can effectively increase the probability of bimolecular recombination (either at the aluminum interface or within the active layer itself). For thicknesses between 15 and 20 nm of MoO<sub>3</sub> more and more of the surface of these rods were covered until there was no direct connection between the active layer and the cathode. The MoO<sub>3</sub> could then act as a full-time hole transporting, electron and exciton blocking layer, which led to a significant increase in  $J_{sc}$ . The open-circuit voltage ( $V_{oc}$ ) of the 20 nm MoO<sub>3</sub> device is increased from 0.223 to 0.555 V, providing further evidence for removal of shunts from the active layer to the aluminum cathode. For device F, a thicker MoO<sub>3</sub> layer will reduce the shunt resistance and caused the mismatch of optical field distribution in active layer,<sup>10,11</sup> which resulted in a decrease in the performance of the device.

The extracted device parameters are summarized in Table I. We can see that the fill factor (FF) of the device increased with the increase of MoO<sub>3</sub> thickness. However, the FF is still very low compared with reported,<sup>12</sup> that is because we get relatively low shunt resistance ( $R_{sh}$ ) due to the presence of electrical shunt paths created by the ZnO nanorod arrays and the voltage dependent carrier recombination created by the rough surface of the ZNR. An extreme drop in  $R_{sh}$  can cause a drop in the  $V_{oc}$  of a solar cell. The fill factor of solar cells can be influenced by the nonzero  $R_s$  and by the finite shunt resistance ( $R_{sh}$ ). According to literature,<sup>13,14</sup>  $R_{sh}$  and  $R_s$  can be independently derived from the slope of the  $I$ - $V$  curve of a solar cell at  $I=I_{sc}$  ( $V=0$ ) and  $V=V_{oc}$  ( $I=0$ ). In this case, as we can see in the Table I, all the devices have an approximate  $R_s$  around 30  $\Omega$ /cm<sup>2</sup>, so we propose that the main influence to the performance of these cells is the  $R_{sh}$ , which can be seen in Fig. 3(b). Increasing the  $R_{sh}$  results in an increase in FF. We should note that even though, in our device, the electron transport layer contains both a 100 nm ZnO seed layer and a 120 nm nanorod array layer, we still can get a higher  $J_{sc}$  than the flat ZnO film device reported in literature<sup>12</sup> that may ascribe to the highly ordered ZNR providing a more direct electron pathway.

A device with a 200 nm ZnO seed layer as the electron selective layer was fabricated, for comparison. The other conditions are same with the 20 nm MoO<sub>3</sub> ZNR device. The

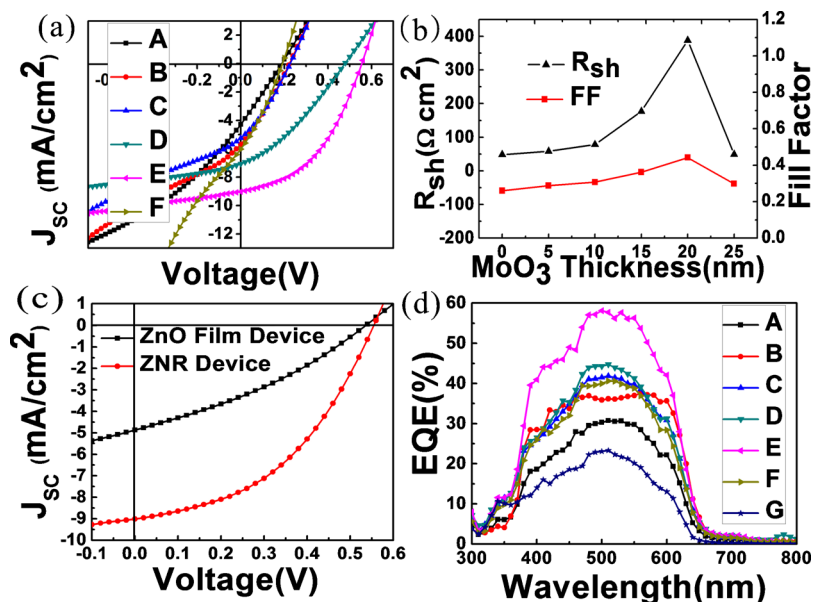


FIG. 3. (Color online) (a)  $J$ - $V$  curve of the ZNR based inverted solar cell with different MoO<sub>3</sub> thickness and (b) the dependence of FF on a  $R_{sh}$ . (c)  $J$ - $V$  curve of ZNR and ZnO film based inverted solar with 20 nm MoO<sub>3</sub> layer. (d) The EQE of both the ZNR with different MoO<sub>3</sub> thickness (ZNR devices) and ZnO film with 20 nm MoO<sub>3</sub> layer devices (ZnO device).

TABLE I. The summary of device performance.

	EF (%)	$V_{oc}$ (V)	$J_{sc}$ (mA/cm <sup>2</sup> )	FF	EQE (%)	$R_{sh}$ ( $\Omega$ cm <sup>2</sup> )	$R_s$ ( $\Omega$ cm <sup>2</sup> )
A	0.203	0.188	4.29	0.260	21.7	48.08	30.35
B	0.394	0.223	6.12	0.288	36.4	58.28	30.26
C	0.367	0.277	5.43	0.307	41.1	78.11	30.29
D	1.06	0.478	6.99	0.326	43.4	176.99	46.87
E	2.15	0.555	9.02	0.442	57.6	387.88	22.17
F	0.343	0.191	6.03	0.298	40.6	49.02	22.44

$J$ - $V$  curve is shown in Fig. 3(c). We can see that the  $V_{oc}$  of the two devices are similar, but the  $J_{sc}$  with only the ZnO film is much lower than the ZNR device, it is reported that the diffusion length of excitons in the conjugated polymer is typically on the order of  $\sim 10$  nm,<sup>15</sup> so the photo generated charge carriers in the 130 nm polymer layer in the ZnO film device are mostly recombined before collection and transport to the electrode in the polymer. Because the gap between two rods are on the order of 10 nm, which is suitable for efficient charge transport, each ZnO nanorod can create a short and continuous pathways for electron transport and increase the contact area between the ZnO nanorod arrays and the organic materials, resulting in a higher photocurrent. Our experimental results confirm this explanation.

The EQE of both the ZNR with different MoO<sub>3</sub> thickness (ZNR devices) and ZnO film with 20 nm MoO<sub>3</sub> layer devices (ZnO device) are shown in Fig. 3(d). The ZNR devices show a maximum EQE of 57.6% at 515 nm. The peak in the EQE spectrum at about 350 nm results from the absorption of the ZnO. With the increased thickness of the MoO<sub>3</sub> layer, a dramatic increase in the EQE is observed of around 36.4%. This increase is likely the result of enhanced charge collection in the device. All of the ZNR devices have a higher EQE than the ZnO device. The EQE spectrum is broader for the ZNR devices in comparison to the ZnO device.

In summary, we studied the effect of the MoO<sub>3</sub> thickness on a ITO/ZNR/P3HT:PCBM/MoO<sub>3</sub>/Al inverted solar cell. We get a maximum efficiency of 2.15% with a 20 nm MoO<sub>3</sub> layer which can effectively improve the interface between the active layer and the Al electrode. Our investigations also show that the vertically oriented, high electron mobility ZNR

arrays can provide continuous electron transport pathways and increase the contact area between the ZNR and the organic materials making the ZNR based solar cell a promising candidate for high efficiency PV devices.

This research was supported by a grant from the U.S. Dept. of Energy under Grant No. DE-FG02-07ER46428 and the AFOSR through Grant No. FA9550-04-1-0161.

- <sup>1</sup>M. P. de Jong, L. J. van IJzendoorn, and M. J. A. de Voigt, *Appl. Phys. Lett.* **77**, 2255 (2000).
- <sup>2</sup>G. K. Mor, S. Kim, M. Paulose, O. K. Varghese, K. Shankar, J. Basham, and C. A. Grimes, *Nano Lett.* **9**, 4250 (2009).
- <sup>3</sup>M. N. Shan, S. S. Wang, Z. Q. Bian, J. P. Liu, and Y. L. Zhao, *Sol. Energy Mater. Sol. Cells* **93**, 1613 (2009).
- <sup>4</sup>J. P. Liu, S. S. Wang, Z. Q. Bian, M. N. Shan, and C. H. Huang, *Chem. Phys. Lett.* **470**, 103 (2009).
- <sup>5</sup>M. S. White, D. C. Olson, S. E. Shaheen, N. Kopidakis, and D. S. Ginley, *Appl. Phys. Lett.* **89**, 143517 (2006).
- <sup>6</sup>D. C. Olson, Y. J. Lee, M. S. White, N. Kopidakis, S. E. Shaheen, D. S. Ginley, J. A. Voigt, and J. W. P. Hsu, *J. Phys. Chem. C* **112**, 9544 (2008).
- <sup>7</sup>D. C. Olson, S. E. Shaheen, R. T. Collins, and D. S. Ginley, *J. Phys. Chem. C* **111**, 16670 (2007).
- <sup>8</sup>V. Shrotriya, G. Li, Y. Yao, C.-W. Chu, and Y. Yang, *Appl. Phys. Lett.* **88**, 073508 (2006).
- <sup>9</sup>M. J. Wang, G. J. Fang, L. Y. Yuan, H. H. Huang, Z. H. Sun, N. S. Liu, S. H. Xia, and X. Z. Zhao, *Nanotechnology* **20**, 185304 (2009).
- <sup>10</sup>D. W. Zhao, P. Liu, X. W. Sun, S. T. Tan, L. Ke, and A. K. K. Kyaw, *Appl. Phys. Lett.* **95**, 153304 (2009).
- <sup>11</sup>D. W. Zhao, S. T. Tan, L. Ke, P. Liu, A. K. K. Kyaw, X. W. Sun, G. Q. Lo, and D. L. Kwong, *Sol. Energy Mater. Sol. Cells* **94**, 985 (2010).
- <sup>12</sup>A. K. K. Kyaw, X. W. Sun, C. Y. Jiang, G. Q. Lo, D. W. Zhao, and D. L. Kwong, *Appl. Phys. Lett.* **93**, 221107 (2008).
- <sup>13</sup>S. S. Hegedus and W. N. Shafarman, *Prog. Photovoltaics* **12**, 155 (2004).
- <sup>14</sup>K. I. Ishibashi, Y. Kimura, and M. Niwano, *J. Appl. Phys.* **103**, 094507 (2008).
- <sup>15</sup>K. M. Coakley and M. D. McGehee, *Chem. Mater.* **16**, 4533 (2004).